Incorporating Temperature-Dependent Mortality into Projected Life Tables

Daniel Precioso[1] (ORCID: 0000-0003-3836-1429)
Francisco J. Suárez Pedraza[1] (ORCID: 0009-0008-6714-2616)
Simon Lloyd[1] (ORCID: 0000-0002-9728-8674)
Carmen Boado-Penas[2] (ORCID: 0000-0002-0643-4921)
David Gómez-Ullate[1] (ORCID: 0000-0002-6890-6584)

[1]School of Science and Technology, IE University
Paseo de la Castellana, 259, 28046 Madrid, Spain

[2]Heriot-Watt University
Edinburgh, Scotland EH14 4AS, United Kingdom

March 2026 (v1.0)

DOI: 10.63537/14417429

Abstract

Climate change may affect mortality patterns through changes in temperature exposure, with potential implications for life tables and life-contingent insurance liabilities. For insurers, the relevant question is not to predict a single future outcome but to understand how alternative climate pathways could impact mortality assumptions and financial results under different scenarios.

This paper presents a methodology for incorporating temperature-dependent mortality into projected life tables at the city level. The approach integrates epidemiological temperature–mortality relationships with standard actuarial mortality projection frameworks while preserving existing actuarial practices. Climate effects are introduced through a transparent, age- and year-specific multiplicative adjustment to baseline all-cause mortality rates.

The framework is explicitly scenario-based. The main contribution of the paper is to show how a projected base life table for a population in a given region can be adjusted to reflect changes in mortality associated with future temperature changes under alternative climate scenarios represented by Representative Concentration Pathways (RCPs). Shared Socioeconomic Pathways (SSPs) describe alternative socioeconomic trajectories and imply much wider variation in demographic outcomes. The aim here is not to adopt the demographic projections associated with a given SSP, but to show how a projected base life table can be modified to account for temperature-related mortality.

Using the city of Bucharest as an illustrative example, the methodology shows how climate-adjusted mortality rates by age and year (and the implied period life tables under each scenario) translate into changes in expected present values of annuities and life insurance contracts (computed on a cohort basis), as well as derived technical provisions (reserves). Impacts vary by age, time, and scenario severity. Uncertainty arising from epidemiological estimation, climate model projections, and adaptation assumptions is propagated through Monte Carlo simulation.

The methodology is intended to support risk assessment and climate-risk sensitivity analysis. Scenario comparisons should be interpreted as illustrating a range of potential impacts on longevity risk and insurance liabilities, rather than identifying a single projected future. Other climate-related factors that affect mortality beyond temperature, such as exposure to emissions, are outside the scope of the present paper and are left for future work.

Contents

1 Introduction **3**

2 The Life Table **4**
2.1 Notation 4
2.2 Methodological Note (Bucharest Baseline) 6
2.3 Mortality Rates and Death Probabilities 6
2.4 Constructing a Period Life Table 6

3 Temperature–Mortality Relative Risk **8**
3.1 Interpolation to Single-Year Ages 9
3.2 Adaptation Scenarios 11
3.3 Adapted Relative Risk Functions 11
3.4 Annual Mean Relative Risk 12

4 Climate-Adjusted Mortality Rate **14**
4.1 The Future World Scenarios 14
4.2 Climate Model Ensemble 15
4.3 How to Adjust the Mortality Rate 16

5 Uncertainty Quantification **19**
5.1 Sources of Uncertainty 19
5.2 Conditional Uncertainty versus Scenario Ranges . . . 20
5.3 Monte Carlo Simulation Pipeline 20

6 Financial Impact **22**
6.1 Constructing a Cohort Life Table 22
6.2 Life-contingent Expected Present Values 22
6.3 Reserves and Financial Impacts 23
6.4 Illustrative Example: Data and Assumptions 23

7 Interpretation and Scope **26**

1. Introduction

This paper presents a methodology for incorporating temperature-dependent mortality into projected life tables for a given city and calendar year. The aim is to integrate epidemiological evidence on temperature–mortality relationships with standard actuarial mortality projection frameworks in a way that is transparent, modular, and directly usable for actuarial pricing, reserving, and climate-risk assessment. In this paper, we use Eurostat projected life tables as the baseline, but the methodology can be applied to any projected life table used by an insurer. Throughout the paper, the city of Bucharest is used as a running illustrative example to demonstrate how the proposed methodology operates in practice, from baseline projected life tables to climate-adjusted mortality tables and financial impacts.

Climate change is introduced through an age- and year-specific **multiplicative adjustment** derived from temperature-dependent relative risk functions and projected temperature distributions. The projected yearly temperature distributions for a given location are obtained from an ensemble of climate models under different RCPs from the Coupled Model Intercomparison Project (CMIP6). The relationship between temperature and mortality is based on epidemiological studies that consider daily time series of deaths and temperatures for a period of 30 years to build relative risk curves for each location and age group [5, 8, 9, 3]. The modelling framework for temperature–mortality relationships is grounded in distributed lag non-linear models (DLNMs) [4], which have been extended to incorporate mortality projection in life insurance contexts [15].

The remainder of the paper is organized as follows: Section 2 presents the construction of actuarial life tables and introduces the notation used throughout the paper. Section 3 introduces temperature–mortality relative risk functions, describes interpolation techniques to single-year ages, and explains how adaptation to heat and cold is accounted for. Section 4 describes how future temperature distributions are obtained under alternative climate scenarios and how relative risks are translated into **climate-adjusted mortality rates**.

Section 5 explains how uncertainty from epidemiological estimates, climate projections, and adaptation assumptions is incorporated into the framework using Monte Carlo simulation. Finally, Section 6 translates climate-adjusted life tables into impacts on products such as annuities, life assurances, as well as technical provisions.

2. The Life Table

A life table[1] summarises how mortality changes with age. Two main types of life tables are commonly distinguished. [7, Ch. 4]:

1. a **cohort life table**, which follows a real birth cohort as it ages through calendar time,
2. a **period life table**, which applies the age-specific death probabilities of a fixed calendar year t to a synthetic cohort.

Unless stated otherwise, the life tables used to represent baseline and climate-adjusted mortality conditions in Sections 2–4 are period life tables indexed by year and region. Cohort calculations (needed for life insurance) are introduced explicitly in Section 6.

Table 1 shows an excerpt of the baseline period life table for Bucharest in 2023, which will be used throughout the document to demonstrate how temperature adjustments affect mortality rates, life tables, and resulting financial outcomes. In the following sections, this Bucharest-based period life table will be adjusted over time to incorporate temperature-dependent mortality effects under alternative climate scenarios.

2.1 Notation

Consider the following variables:

- x denotes the exact age (in years) of an individual,
- t denotes the calendar year,
- g denotes a region (city or country).

Throughout, subscripts x, t, g denote age, calendar year, and region. We use:

- $E_{x,t,g}$: exposure at age x (person-years, often approximated by mid-year population) in year t for region g,
- $D_{x,t,g}$: # of observed deaths at age x in year t for region g,
- $m_{x,t,g}$: central death rate at age x in year t for region g, with $m_{x,t,g} = D_{x,t,g}/E_{x,t,g}$,
- $q_{x,t,g}$ probability that an individual aged x exact in year t for region g dies before reaching age $x+1$,
- $\ell_{x,t,g}$: number of individuals alive at exact age x in time t for region g in a synthetic cohort (radix $\ell_{0,t,g} = 100{,}000$),
- $d_{x,t,g}$: number of deaths between exact ages x and $x+1$ for region g.

When presenting the Bucharest 2023 baseline table, we suppress the year and region subscripts for readability. We retain the region subscript in the definitions above, but otherwise suppress

[1] Throughout the report we use the words life table and mortality table interchangeably

Table 1: Bucharest Municipality period Life Table, 2023 (unisex), with selected ages illustrated. This life table was computed using PCLM (Penalized Composite Link Model) ungrouping of 5-year age group data. Data sources: INS TEMPO POP106A (population) and POP206K (deaths) for Bucharest Municipality, 2023.

Age x	Prob. of dying q_x	Survivors ℓ_x	Life expectancy e_x
0	0.000 89	100 000	77.16
1	0.000 67	99 911	76.23
5	0.000 24	99 723	72.37
10	0.000 13	99 633	67.43
15	0.000 15	99 568	62.47
20	0.000 32	99 467	57.53
25	0.000 51	99 263	52.64
30	0.000 60	98 995	47.78
35	0.000 87	98 656	42.94
40	0.001 56	98 109	38.16
45	0.002 41	97 180	33.50
50	0.004 18	95 749	28.96
55	0.007 04	93 219	24.67
60	0.010 96	89 381	20.62
65	0.017 49	83 549	16.87
70	0.027 52	75 075	13.48
75	0.039 56	63 743	10.41
80	0.064 48	49 922	7.58
85	0.104 84	32 914	5.18

it in the text and formulas for clarity. In Section 2.4 we also fix a given year t and write $q_x, \ell_x, d_x, L_x, e_x$ to simplify the period-table formulas.

2.2 Methodological Note (Bucharest Baseline)

The Bucharest life table was constructed using the Penalised Composite Link Model (PCLM) method [14] to disaggregate 5-year age-group data into single-year age estimates. The input data consisted of:

- Population by 5-year age groups: INS TEMPO POP106A (Bucharest Municipality, 2023).
- Death counts by 5-year age groups: INS TEMPO POP206K (Bucharest Municipality, 2023).

The PCLM method uses penalised B-splines to estimate a smooth underlying distribution from coarsely grouped counts, preserving the total counts while providing single-year disaggregation.

The period life expectancy shown in Table 1 is slightly higher than the values from the Romanian National Institute of Statistics (INS). This difference arises because INS calculates life expectancy using population and deaths averaged over a three-year period [10], which includes the effects of COVID-19. In contrast, our calculations consider only the 2023 population and deaths, and therefore do not reflect the impact of COVID-19.

2.3 Mortality Rates and Death Probabilities

The initial mortality rate q_x at age x can be calculated using the central mortality rate as follows [12]:

$$q_{x,t} = \frac{m_{x,t}}{1 + (1 - a_x) \times m_{x,t}} \tag{1}$$

where a_x is the average fraction of the year lived by individuals who die between ages x and $x + 1$. We take $a_0 = 0.1$ for age 0 (infants), because newborn deaths tend to occur during their first weeks [12]. For other ages, a_x is treated as age-specific; in the numerical example we use $a_x = 0.5$ for ages 1–84 and $a_x = 0.4$ for ages 85+ to reflect the higher concentration of deaths earlier in the year at advanced ages.

2.4 Constructing a Period Life Table

A period life table summarises mortality conditions in a given calendar year t by applying the set of age-specific one-year death probabilities $\{q_{x,t}\}_{x \geq 0}$ to a synthetic cohort.

Let $q_{x,t} \in [0, 1]$ be the one-year probability of death between ex-

act ages x and $x+1$ in year t, obtained from a standard actuarial mortality projection model. The baseline mortality model is calibrated on historical mortality data and implicitly reflects historical climate conditions.

Let e_x denote the curtate life expectancy of an individual aged x, i.e., the expected number of completed years remaining by the individual. Mathematically,

$$e_x = \sum_{k=1}^{\infty} {}_kp_x. \tag{2}$$

where ${}_kp_x$ is the probability that an individual aged x survives for at least k additional years, given by

$${}_kp_x = \prod_{j=0}^{k-1}(1 - q_{x+j})$$

The complete life expectancy for an individual aged x,$\mathring{e}_x$, can be calculated by the approximated equation:

$$\mathring{e}_x \approx e_x + a_x. \tag{3}$$

In practice, the sum is finite: the terminal (limiting) age is denoted ω, with $q_{\omega-1} = q_\omega = \cdots = 1$.

3. Temperature–Mortality Relative Risk

This section describes the epidemiological inputs used to adjust baseline all-cause mortality for temperature effects, independently of climate scenarios. Building on the Bucharest baseline period life table introduced in Section 2, we introduce temperature–mortality relative risk functions that quantify how mortality rates vary with daily temperature. Operationally, these functions generate temperature-dependent climate mortality adjustment factors that will later be combined with baseline mortality rates $m_{x,t}$ to build climate-adjusted period life tables (year-by-year slices indexed by t). Climate pathways are introduced later, when projecting temperature distributions in Section 4. As above, the region subscript g is suppressed for readability, but remains part of the underlying definitions.

For a fixed region (omitted for clarity) and age group h, epidemiological studies [8] provide relative risk functions dependent on temperature.

$$\mathrm{RR}_h(T) \in (0, \infty),$$

where T denotes the mean daily temperature.

Relative risks are defined with respect to a reference temperature T_h^* (often the minimum mortality temperature) such that

$$\mathrm{RR}_h(T_h^*) = 1.$$

These so-called exposure-response functions (ERFs) capture excess mortality associated with both cold and heat exposure. ERFs are typically estimated using distributed lag non-linear models (DLNM) [4]. Figure 1 shows the temperature–mortality exposure–response functions for the city of Bucharest, by age group, estimated using the methodology of [9]. Note that the curve for the youngest group tends to dip below 1 for extremely cold temperatures. This is an artefact of the spline due to the lack of mortality data for the young population. When the reference temperature T_h^* corresponds to the minimum mortality temperature, the theoretical relationship satisfies $\mathrm{RR}_h(T) \geq 1$; in practice, estimated curves may violate this constraint in poorly informed tails, and values below 1 should be interpreted as estimation noise.

Relative risk modifies the mortality rate. Given a mortality rate estimated at temperature A, we can compute the mortality rate for the same group at temperature B as [8]

$$m_{h,t}^{\mathsf{B}} = m_{h,t}^{\mathsf{A}} \times \frac{\mathrm{RR}_h(T^{\mathsf{B}})}{\mathrm{RR}_h(T^{\mathsf{A}})}\,. \tag{4}$$

Equation (4) formalises how temperature-dependent relative risks modify baseline mortality rates and will be used in Section 4

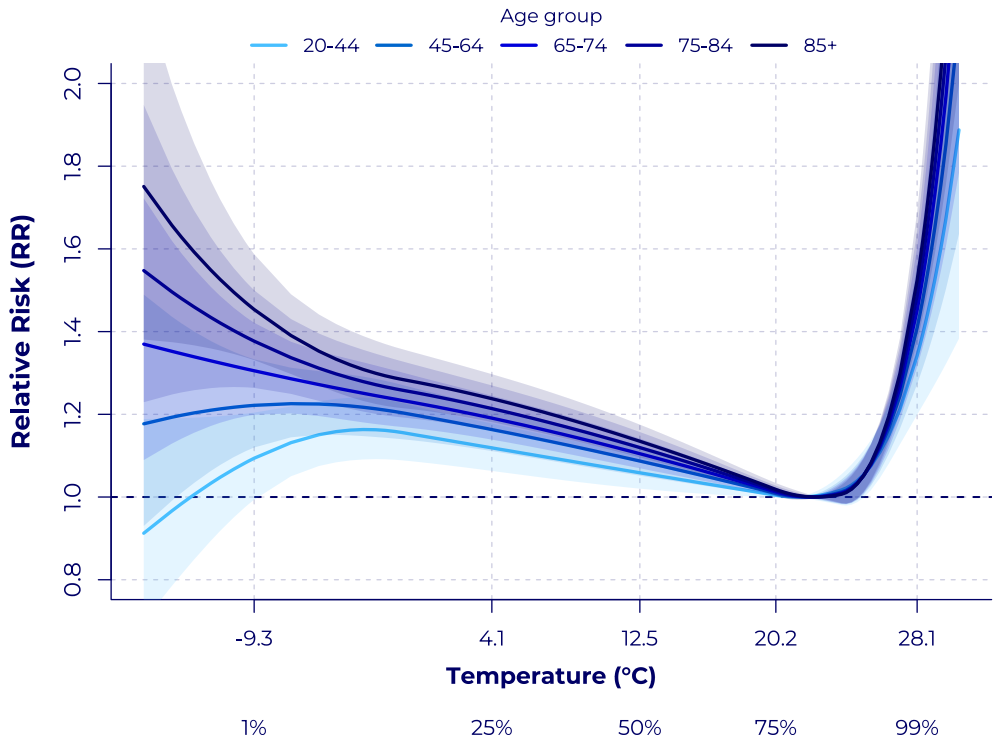

Figure 1: Temperature–mortality exposure–response functions (relative risk versus mean daily temperature) for the city of Bucharest (Romania), shown by age group. Shaded bands represent 95% confidence intervals. Source: [9].

to construct climate-adjusted period life tables for the Bucharest example.

3.1 Interpolation to Single-Year Ages

Relative risk functions are available for a finite number of age groups, as shown in Figure 1. To apply temperature-dependent mortality adjustments to the single-year life tables introduced for Bucharest in Section 2, these relative risk curves must be interpolated by age.

Let $\bar{x}_h$ denote a representative age for group h. For each temperature T, define the excess risk:

$$\mathrm{ER}_h(T) = \mathrm{RR}_h(T) - 1. \tag{5}$$

Working with excess risk rather than relative risk ensures that interpolation preserves the reference temperature at which mortality is minimised.

For fixed T, the quantity

$$\log\big(\mathrm{ER}_h(T) + \varepsilon\big),$$

with a small constant $\varepsilon > 0$, is interpolated throughout the age using a monotone or piecewise-linear interpolation scheme. This yields age-specific excess risks $\mathrm{ER}_x(T)$ and the corresponding single-year relative risks:

$$\mathrm{RR}_x(T) = 1 + \mathrm{ER}_x(T). \tag{6}$$

By construction, the interpolation preserves the anchoring at the reference temperature (minimum mortality), so that $\mathrm{RR}_x(T_x^*) = 1$ for all ages. For the central age within the group, $\hat{x}_h$, we consider $\mathrm{RR}_{\hat{x}_h}(T) = \mathrm{RR}_h(T)$. Figure 2 illustrates the result of this interpolation for the Bucharest example, producing a smooth relative risk surface in both age and temperature. This age–temperature relative risk surface forms the basis for the age-specific climate mortality adjustment factors illustrated later in Figure 5.

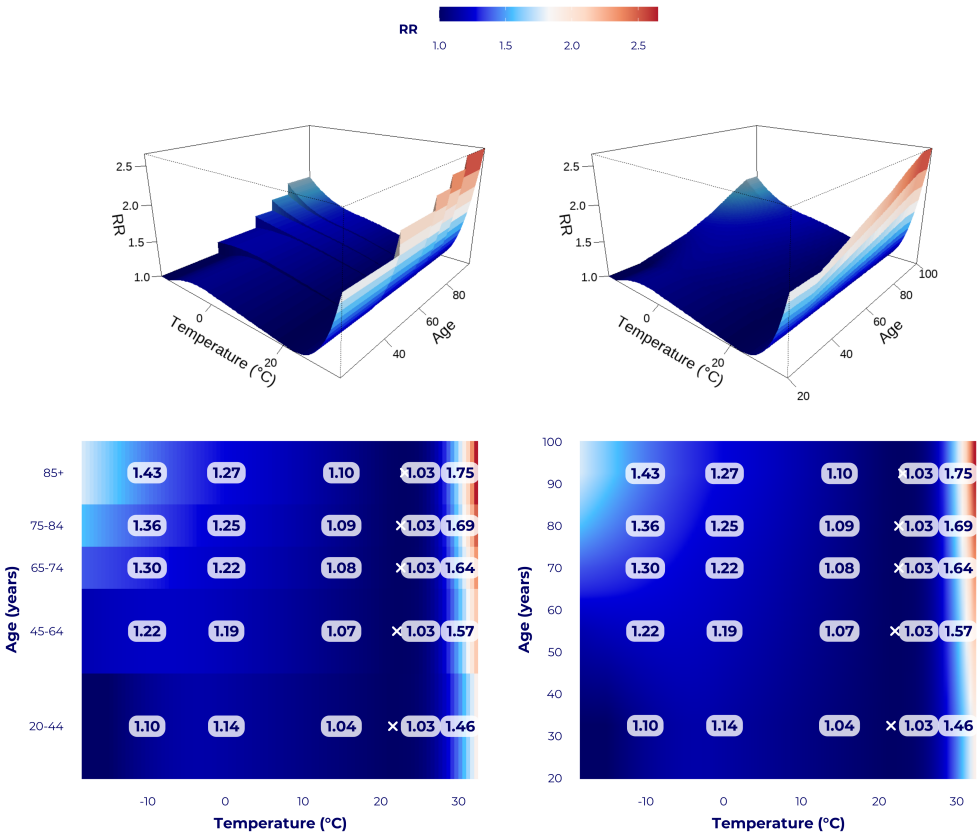

Figure 2: Interpolated temperature–mortality exposure–response surface for the city of Bucharest, showing relative risk as a function of both age and mean daily temperature. The surface is obtained by interpolating age-group-specific exposure–response functions to single-year ages, ensuring consistency with the single-year life table framework.

3.2 Adaptation Scenarios

Temperature–mortality relationships estimated from historical data reflect the level of adaptation prevailing during the estimation period (e.g., housing quality, access to cooling and heating, health system responses, and behavioural changes). Future adaptation may reduce the excess mortality associated with exposure to temperature, particularly in extreme heat [8].

To represent adaptation in a transparent and interpretable way, we introduce a scenario-based adaptation mechanism that progressively discounts the excess temperature-related risk over time.

For each age x, we define two adaptation parameters:

- $A_x^H \in [0, 1]$: final degree of adaptation to **heat-related** mortality by the year 2100,
- $A_x^C \in [0, 1]$: final degree of adaptation to **cold-related** mortality by the year 2100.

These parameters are interpreted as percentages of excess risk removed:

- $A = 0$ corresponds to no adaptation (0% of excess risk removed),
- $A = 1$ corresponds to complete adaptation (100% excess risk removed, which is equivalent to RR $= 1$).

Therefore, each relative risk curve is fully characterised by the pair (A_x^H, A_x^C).

Let $t_0 = 2020$ denote the initial year and $t_f = 2100$ the final year. Adaptation is assumed to increase linearly over time from zero in year t_0 to its final level in year t_f.

Define the time-dependent adaptation functions:

$$A_x^H(t) = A_x^H \times \frac{t - t_0}{t_f - t_0}, \qquad A_x^C(t) = A_x^C \times \frac{t - t_0}{t_f - t_0}, \tag{7}$$

with $A_x^H(t) = A_x^C(t) = 0$ for $t \leq t_0$ and $A_x^H(t) = A_x^H$, $A_x^C(t) = A_x^C$ for $t \geq t_f$.

3.3 Adapted Relative Risk Functions

Let $\text{RR}_x(T)$ denote the baseline temperature–mortality relative risk function, centred at the reference temperature T_x^* such that $\text{RR}_x(T_x^*) = 1$.

Define the adapted relative risk function for year t as:

$$\mathrm{RR}_x^{\mathrm{ad}}(T,t) = \begin{cases} 1 + \big(1 - A_x^H(t)\big)\big(\mathrm{RR}_x(T) - 1\big), & T > T_x^*, \\ 1 + \big(1 - A_x^C(t)\big)\big(\mathrm{RR}_x(T) - 1\big), & T < T_x^*. \\ 1, & T = T_x^*. \end{cases} \tag{8}$$

By construction:

- the relative risk remains anchored at $\mathrm{RR}_x^{\mathrm{ad}}(T_x^*, t) = 1$ for all t,
- excess risk is progressively reduced over time,
- Adaptation to heat and cold can differ in magnitude.

Therefore, each calendar year t is associated with a distinct adaptation-adjusted relative risk curve. The adapted relative risk functions $\mathrm{RR}_x^{\mathrm{ad}}(T,t)$ replace $\mathrm{RR}_x(T)$ in the calculation of:

- annual mean relative risks,
- population attributable fractions,
- climate mortality adjustment factors.

All subsequent steps of the construction of the climate-adjusted period life table remain unchanged.

3.4 Annual Mean Relative Risk

Let $T_{t,d}$ denote the daily mean temperature on day d of year t, obtained from the projections of the bias-corrected climate model.

Define the empirical temperature distribution (histogram) for year t as:

$$H_t(T) = \frac{1}{\mathrm{ND}_t} \sum_{d=1}^{\mathrm{ND}_t} \mathbf{1}\{T_{t,d} = T\}, \tag{9}$$

where ND_t is the number of days in year t. The formula $\mathbf{1}\{\cdot\}$ is 1 when the expression inside the curly brackets is true, and 0 otherwise. In other words, equation (9) counts the ratio of days in which the average temperature was T (assuming that we record temperature T in integer Celsius degrees).

For each age x and year t, define the annual mean relative risk:

$$\overline{\mathrm{RR}}_{x,t} = \sum_T H_t(T)\, \mathrm{RR}_x^{\mathrm{ad}}(T,t). \tag{10}$$

This quantity summarises the average mortality risk at age x induced by the annual temperature distribution. Figure 3 presents a visualisation of a relative risk curve lying on top of two temperature distributions that belong to different years for the same region.

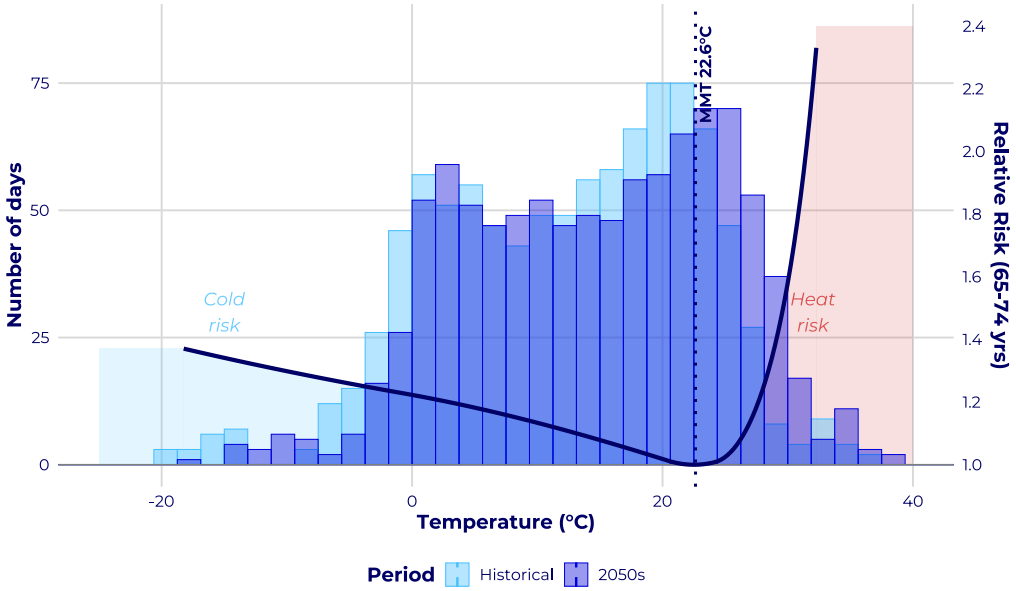

Figure 3: Histogram of average daily temperatures in Bucharest (Romania). Blue represents historical temperatures from 2000–2014, while purple showcases a projected distribution for the 2050s (2050–2059) under Representative Concentration Pathway (RCP) 7.0. The dark blue curve represents the temperature-related relative risk exposure-response function for Bucharest citizens between 65 and 74 years old. The green dark blue vertical line indicates the minimum mortality temperature (MMT) at 22.6°C, separating cold risk (left) from heat risk (right).

Aggregation approximation. The climate mortality adjustment factor is computed using the annual mean relative risk $\overline{\text{RR}}_{x,t}$, which averages the daily temperature-dependent relative risk over the year. A more granular approach would apply the relative risk to daily baseline mortality and aggregate to annual totals. However, this would require daily baseline mortality data, which is not typically available in actuarial applications. The annual averaging approximation is common in the climate-health literature [5, 8] and is expected to introduce minimal bias when the relative risk function is approximately linear over the range of temperatures that occur with high frequency. Sensitivity to this approximation could be assessed by comparing results with and without weighting by seasonal mortality patterns, where such data are available.

4. Climate-Adjusted Mortality Rate

4.1 The Future World Scenarios

To incorporate climate change into projected life tables, it is necessary first to characterise the temperature distribution of each region of interest. Several data sources can be used for this purpose, depending on whether historical or future temperatures are considered.

For historical temperature data, we rely on the European Centre for Medium-Range Weather Forecasts **(ECMWF) Reanalysis version 5 (ERA5)** [6]. ERA5 provides globally consistent reanalysis data for near-surface (2 m) air temperature at an hourly temporal resolution and a spatial resolution of $0.25°$, with coverage extending back to 1940. For each region, we spatially aggregate ERA5 grid cells intersecting the relevant polygon and compute an area-weighted average, producing a single daily temperature observation $T_{t,d}$ for each day d of the calendar year $t \leq 2025$.

Projecting future temperatures introduces additional complexity, as temperature trajectories depend on alternative climate-change scenarios. These scenarios are commonly defined using **Representative Concentration Pathways (RCPs)**, which specify alternative trajectories of radiative forcing (measured in W/m^2) by the year 2100 [16]. Higher forcing levels correspond to higher greenhouse gas concentrations and, consequently, stronger climate change.

Shared Socioeconomic Pathways (SSPs) were introduced in 2014, building on earlier SRES narratives (2000), and describe alternative trajectories of socioeconomic development, including population growth, economic activity, technological change, and inequality [13]. In CMIP6, RCPs and SSPs are combined to create internally consistent scenario families. Although SSP and RCP are conceptually independent and can, in principle, be combined flexibly, a limited set of SSP–RCP combinations is commonly used in practice. Table 2 summarises the combinations most frequently adopted in the literature.

In parallel, the **Network for Greening the Financial System (NGFS)** has developed a set of climate scenarios designed specifically for financial risk assessment and stress testing, with a focus on both transition and physical climate risks [11]. NGFS scenarios are built using SSPs and RCPs and translate alternative climate pathways into macroeconomic and financial variables suitable for use in supervisory exercises such as ORSA. The present work complements the NGFS framework by providing a quantitative link between physical climate risk and age-specific mortality, allowing the assessment of climate impacts on life insurance and annuity liabilities. Actuarial climate indices designed to cap-

ture the financial relevance of climate variables, such as those proposed for the Iberian Peninsula [17], illustrate the growing interest in translating physical climate signals into insurance-relevant metrics.

Table 2: Representative Concentration Pathways (RCPs), their most commonly used Shared Socioeconomic Pathway (SSP) counterparts, and approximate mappings to NGFS climate scenarios. The final column reports indicative ranges of end-of-century (EoC) global mean surface temperature increase relative to pre-industrial levels. Associations are approximate and based on consistency of radiative forcing and policy assumptions.

RCP	SSP	NGFS scenario(s)	EoC (°C)
2.6	SSP1 (Sustainability)	Net Zero 2050 Low Demand	1.3–2.4
4.5	SSP2 (Middle of the road)	Below 2°C Delayed Transition	2.1–3.5
7.0	SSP3 (Regional rivalry)	Fragmented World NDCs	2.8–4.6
8.5	SSP5 (Fossil-fuelled develop.)	Current Policies	3.3–5.7

4.2 Climate Model Ensemble

Future temperatures are obtained from an ensemble of climate model projections. Specifically, for each RCP–SSP scenario, we use daily temperature outputs from 21 combinations of global and regional climate models, consisting of general circulation models (GCMs) and, where applicable, their regional downscalings via regional climate models (RCMs), as described in [8, 9].

Each climate model within the ensemble provides a physically consistent but distinct realisation of future daily temperatures, reflecting differences in model structure, parameterisation, and internal climate variability. Rather than selecting a single model or averaging temperatures across models at each point in time, we treat all model outputs within a given scenario as equally plausible representations of future climate conditions.

Figure 4 illustrates this ensemble structure for the city of Bucharest, showing how alternative climate model projections diverge under different RCP scenarios and how this spread motivates the use of a pooled temperature distribution.

Operationally, for each calendar year t, the daily temperatures of all models are pooled to form a single empirical temperature

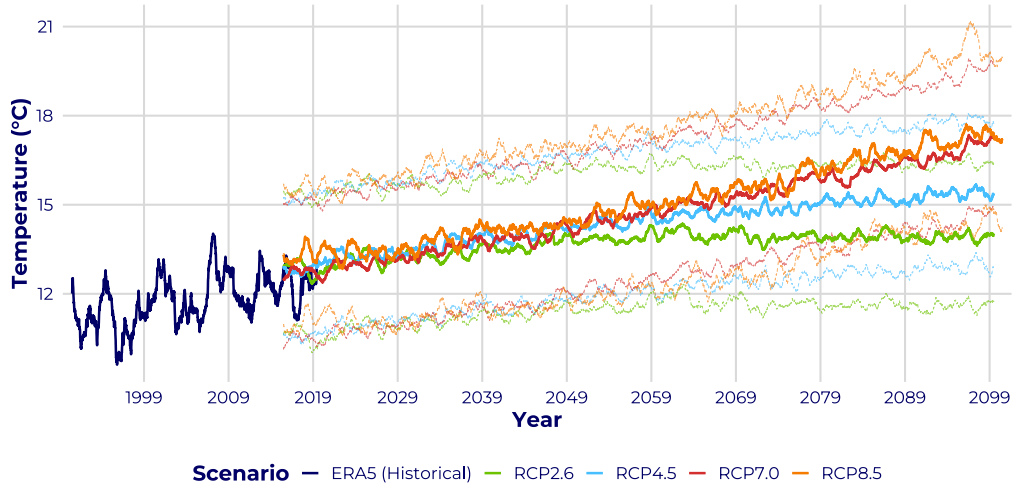

Figure 4: Projected temperature trajectories for the city of Bucharest (Romania) under alternative climate scenarios. Solid lines represent 365-day moving averages of daily mean temperature, computed separately for each Representative Concentration Pathway (RCP). Dashed lines indicate the 25th and 75th percentiles across the 19 climate model projections (GCM ensemble), reflecting climate-model uncertainty rather than statistical confidence intervals. Historical observations (1991–2020) are from ERA5 reanalysis data.

distribution conditional on the chosen scenario. This pooled distribution represents the range of temperatures consistent with the scenario assumptions and the underlying uncertainty of the climate-model. The annual temperature distributions $H_t(T)$ are then constructed from this combined sample, and all subsequent mortality calculations are based on samples from this distribution.

This approach allows climate model uncertainty to be propagated transparently into mortality and financial outcomes, while avoiding reliance on any single climate model.

4.3 How to Adjust the Mortality Rate

Standard actuarial mortality projection models implicitly assume that future mortality evolves in line with historical experience, without explicitly accounting for shifts in the temperature distribution driven by climate change. To incorporate climate effects, we compute the annual mean temperature-related relative risk under each scenario (RCP–SSP pathway). The historical reference period $\mathcal{H}$ is set to match the calibration window of the baseline mortality model (e.g., 1990–2019 in the Bucharest example). This ensures that climate effects already embedded in historical mortality are not double-counted in the adjustment.

For each age x and calendar year t, we summarise temperature-related mortality using the annual mean relative risk $\overline{\text{RR}}_{x,t}$ defined in Section 3.4. When adaptation is included, $\overline{\text{RR}}_{x,t}$ is computed using the adapted curve $\text{RR}_x^{\text{ad}}(T,t)$. We then define a multiplicative **climate mortality adjustment factor** by normalising this annual mean relative risk to the historical reference period $\mathcal{H}$:

$$\widetilde{M}_{x,t} = \frac{\overline{\text{RR}}_{x,t}}{\frac{1}{|\mathcal{H}|}\sum_{s\in\mathcal{H}} \overline{\text{RR}}_{x,s}}. \tag{11}$$

By construction, the normalised adjustment factor $\widetilde{M}_{x,t}$ averages to one over the historical reference period, ensuring consistency with the baseline mortality rates by age and year.

This is an annual adjustment: $\overline{\text{RR}}_{x,t}$ averages daily relative risks throughout the year (via the temperature distribution), and $m_{x,t}^{\text{ref}}$ is treated as an annual central death rate consistent with the life-table time step. Intra-annual seasonality in baseline mortality and potential seasonality in susceptibility are therefore not modelled explicitly. A more granular alternative would apply the relative risk day by day and then aggregate to an annual rate; for annual life-table quantities, the literature typically treats this approximation as negligible relative to other sources of uncertainty, and we adopt the same convention [8].

The climate-adjusted central death rate is then defined as

$$m_{x,t}^{\text{clim}} = m_{x,t}^{\text{ref}} \times \widetilde{M}_{x,t}. \tag{12}$$

Here, $m_{x,t}^{\text{ref}}$ denotes the reference mortality rate calibrated on historical mortality data, which implicitly reflects historical climate conditions. Normalisation in equation (11) is therefore essential to isolate the incremental effect of future temperature changes.

The corresponding one-year death probability is obtained using the standard life-table relationship in equation (1),

$$q_{x,t}^{\text{clim}} = \frac{m_{x,t}^{\text{clim}}}{1 + (1 - a_x) \times m_{x,t}^{\text{clim}}}. \tag{13}$$

Together, these quantities define a climate-adjusted period life table for year t. Repeating this construction across projection years yields climate-adjusted mortality rates by age and year $\{q_{x,t}^{\text{clim}}\}$: fixed-$t$ slices correspond to period life tables, while cohort calculations needed for expected present values (EPVs) follow the diagonal $(x+j, t+j)$ as formalised in Section 6. All standard

actuarial quantities (including period life expectancy, life annuity values, life insurance values, and reserves) are subsequently computed from the relevant period table or cohort construction, using these climate-adjusted death probabilities.

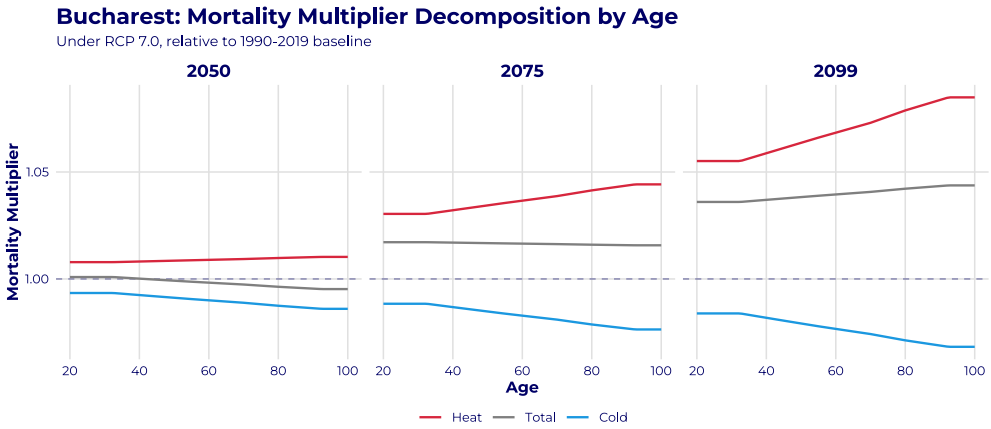

Figure 5: Projected mortality multiplier for Bucharest under RCP 7.0, relative to the 1990–2019 baseline. Lines represent the mean across 19 CMIP6 climate models. The horizontal dashed line at 1.0 marks the baseline level. The mortality multiplier $\widetilde{M}_{x,t}$ is computed as the ratio of projected annual mean relative risk to the historical baseline, using temperature–mortality exposure–response functions from [8, 9]. Heat and cold specific multipliers are also shown.

Figure 5 illustrates the age-specific climate mortality adjustment factor for the Bucharest example, showing how the impact of temperature on mortality varies over ages and evolves over time under a given climate scenario. RCP 7.0 is used here as a representative climate pathway for illustrative purposes; analogous figures can be produced for alternative scenarios using the same methodology.

In addition, Figure 5 shows the mortality multiplier specific to heat and cold temperatures. The multiplier is computed as follows:

$$\overline{\mathrm{RR}}^{\mathrm{cold}}_{x,t} = \sum_{T<T^*_x} H_t(T)\,\mathrm{RR}^{\mathrm{ad}}_x(T,t) + \sum_{T\geq T^*_x} H_t(T) \tag{14}$$

$$\overline{\mathrm{RR}}^{\mathrm{heat}}_{x,t} = \sum_{T<T^*_x} H_t(T) + \sum_{T\geq T^*_x} H_t(T)\,\mathrm{RR}^{\mathrm{ad}}_x(T,t) \tag{15}$$

Equation (15) implies that when computing the heat risk, any day with temperatures below the minimum mortality temperature T^*_x is taken as a risk of 1 (i.e., cold does not have any effect). The opposite is true for the cold risk. Recall that $H_t(T)$ is

computed by the following equation (9). Equation (15) defines temperature-specific relative risks, not the mortality multipliers. The corresponding heat- and cold-specific multipliers are obtained by applying the normalisation in equation (11) to $\overline{\mathrm{RR}}^{\mathrm{heat}}_{x,t}$ and $\overline{\mathrm{RR}}^{\mathrm{cold}}_{x,t}$, respectively. For rigour, it is immediately necessary to prove that:

$$\overline{\mathrm{RR}}_{x,t} = \overline{\mathrm{RR}}^{\mathrm{cold}}_{x,t} + \overline{\mathrm{RR}}^{\mathrm{heat}}_{x,t} - 1$$

For instance, in 2075 the mortality multiplier for age 60 is 1.02, which means 2% extra deaths due to the change in temperature. Note that cold-related deaths have a multiplier below 1, signalling that global warming will produce fewer cold related deaths in 2075. For Bucharest, Figure 5 suggests a marked increase in heat-related mortality (reaching about 9% at times) alongside a decrease in cold-related mortality (down to about -4%). These opposing effects yield a modest net adjustment in the overall multiplier. This decomposition is informative and warrants separate investigation, although the remainder of the document focuses on the combined effect.

5. Uncertainty Quantification

This section describes how uncertainty can be propagated through the temperature-adjustment framework and how uncertainty intervals can be obtained for climate-adjusted period life tables (year-by-year slices) and for downstream cohort-based actuarial quantities such as expected present values (EPVs) of annuities and life assurances.

5.1 Sources of Uncertainty

We distinguish four conceptually distinct sources of uncertainty.

1. **Epidemiological uncertainty (relative risk functions).** Temperature–mortality relationships are estimated from historical data (e.g., using distributed lag non-linear models), which produces uncertainty in the relative risk functions $\mathrm{RR}_h(T)$ and, after age interpolation, in $\mathrm{RR}_x(T)$.
2. **Uncertainty of climate projection.** The uncertainty in daily temperature projections $T_{t,d}$ arises from structural differences between climate models (GCMs/RCMs) and internal climate variability, both of which are represented through the multi-model ensemble described in Section 4.
3. **Uncertainty of the baseline mortality projection.** The insurer's baseline mortality rates by age and year (e.g. obtained from Lee–Carter or mortality improvement models)

are themselves subject to parameter and process uncertainty. In the simplest implementation, this baseline can be treated as fixed if only a point estimate $q_{x,t}^{\text{ref}}$ is provided.

4. **Adaptation uncertainty.** Future adaptation to heat and cold is not statistically identifiable from current data and is therefore treated as scenario uncertainty, represented by alternative values of the adaptation parameters (A_x^H, A_x^C).

5.2 Conditional Uncertainty versus Scenario Ranges

To ensure interpretability, we distinguish between two types of uncertainty assessment.

- **Conditional uncertainty intervals**, obtained by fixing the climate pathway (e.g. RCP) and adaptation parameters (A^H, A^C), and propagating epidemiological and climate-model uncertainty through the framework.
- **Scenario ranges**, obtained by repeating the conditional analysis across multiple RCPs and/or adaptation parameter values. These ranges reflect deep uncertainty and should not be interpreted as probabilistic confidence intervals.

The discussion below distinguishes conditional uncertainty intervals from scenario ranges. The illustrative numerical results in Section 6.4 are point estimates.

5.3 Monte Carlo Simulation Pipeline

Uncertainty propagation is implemented via Monte Carlo simulation. For simulation runs $r = 1, \ldots, R$, the following steps are performed.

Step 1: Sampling relative risk functions. The parameters of the epidemiological model (e.g. spline coefficients of the DLNM) are sampled to obtain a simulated relative risk function $\text{RR}_h^{(r)}(T)$ for each age group. These curves are interpolated across age as described in the deterministic framework to obtain single-year functions $\text{RR}_x^{(r)}(T)$.

Step 2: Sampling temperature trajectories. A climate model member is selected and internal variability is sampled to obtain daily temperatures $T_{t,d}^{(r)}$ for each projection year t. The corresponding annual temperature distribution $H_t^{(r)}(T)$ is constructed.

Step 3: Applying adaptation scenarios. For the chosen adaptation scenario (A^H, A^C), year-specific adapted relative risk curves

$$\text{RR}_x^{\text{ad},(r)}(T, t)$$

are constructed using the linear time-evolution of adaptation from 2020 to 2100, as defined in the adaptation section. Therefore, each calendar year is associated with a distinct relative risk curve.

Step 4: Calculation of annual mean relative risk and climate mortality adjustment factors. The annual mean relative risk is computed as

$$\overline{\mathrm{RR}}_{x,t}^{(r)} = \sum_{T} H_t^{(r)}(T)\, \mathrm{RR}_x^{\mathrm{ad},(r)}(T,t). \tag{16}$$

From this quantity, we calculate the normalised climate mortality adjustment factor $\widetilde{M}_{x,t}^{(r)}$ from equation (11).

Step 5: Constructing climate-adjusted mortality rates by age and year. The simulated adjustment factor is applied to the reference mortality rates following the equation (12) and converted to the probability of death at one-year $q_{x,t}^{\mathrm{clim},(r)}$.

Step 6: Computing actuarial quantities. Using the simulated mortality rates by age and year $q_{x,t}^{\mathrm{clim},(r)}$, period life tables can be obtained for any fixed valuation year t. For each valuation age x and year t of interest, cohort survival probabilities are then constructed along $(x+j, t+j)$ and the actuarial quantities of interest (e.g., EPVs of annuities or life assurances, reserves) are computed using standard actuarial formulas.

The Monte Carlo procedure yields an empirical distribution for each output of interest, including age-specific mortality rates and actuarial present values. Uncertainty intervals are obtained from empirical quantiles of these distributions, for example the 2.5% and 97.5% quantiles to form a 95% confidence interval.

If baseline mortality uncertainty is included, the pipeline can be extended by sampling baseline-projection parameters (e.g. Lee–Carter mortality indices) within the Monte Carlo loop, yielding joint uncertainty in baseline mortality and climate adjustment.

6. Financial Impact

This section translates climate-adjusted projected life tables into financial impacts on life-contingent products. Using these life tables, we first construct a cohort life table and then calculate life annuities, life assurance, and technical provisions.

6.1 Constructing a Cohort Life Table

To compute expected present values of life-contingent cash flows, we construct a cohort life table. A cohort life table follows the same birth cohort as it ages through future calendar years, and therefore incorporates the full projected path of mortality (baseline mortality improvements and climate adjustments) over the insured's remaining lifetime. This contrasts with the period life table of Section 2.4, which assumes a constant mortality rate for age x over time.

We consider two mortality bases: the reference rates $q^{\text{ref}}_{x,t}$ (without climate adjustment) and the climate-adjusted rates $q^{\text{clim}}_{x,t}$. The latter are derived from the former using the climate adjustment procedure described in Section 4.

As in Section 2.4, we define the cohort life-table quantities in the same order, but evaluated along the diagonal $(x+k, t+k)$. The notation and interpretation mirror Section 2.4; only the indexing changes to follow the cohort path. Let $q^{(b)}_{x+k,\,t+k}$ be the one-year death probability at age $x+k$ in year $t+k$ under basis b.

The cohort survival probabilities for an individual aged x in year t are

$$ {}_kp^{(b)}_{x,t} = \prod_{j=0}^{k-1} \left(1 - q^{(b)}_{x+j,\,t+j}\right), \qquad k \geq 1, \tag{17} $$

with ${}_0p^{(b)}_{x,t} = 1$.

6.2 Life-contingent Expected Present Values

Two standard life-contingent products are considered: life annuities and life insurance contracts. In both cases, expected present values (EPVs) are calculated under both reference and climate-adjusted rates.

Let i be the annual effective interest rate and $v = (1+i)^{-1}$ the discount factor.

Life Annuity: The EPV at age x and year t under basis b for a life annuity-due, which pays 1 unit at the beginning of each year while the individual aged x is alive, is given by:

$$ \ddot{a}^{(b)}_{x,t} = \sum_{k=0}^{\infty} v^k \, {}_kp^{(b)}_{x,t} \, . \tag{18} $$

For annual payments c_k at time k (conditional on survival), the EPV is

$$\sum_{k=0}^{\infty} v^k \, c_k \, {}_kp_{x,t}^{(b)} \, . \tag{19}$$

The corresponding climate adjusted EPV of the life annuity $\ddot{a}_{x,t}^{(\text{clim})}$ is obtained from (18) by replacing the base survival probability $p_{x,t}^{(b)}$ with the climate modified one $p_{x,t}^{(\text{clim})}$ from (17), using (12) and (13).

Life Insurance (Assurance): The EPV at age x and year t under basis b for a life insurance, which pays 1 unit at the end of the year of death for an individual who is now x, is given by:

$$A_{x,t}^{(b)} = \sum_{k=0}^{\infty} v^{k+1} \, {}_kp_{x,t}^{(b)} \, q_{x+k,\,t+k}^{(b)} \, . \tag{20}$$

For a level death benefit S, the EPV is $S \, A_{x,t}^{(b)}$.

As explained above, the climate adjusted EPV of the Life Assurance $A_{x,t}^{(\text{clim})}$ is calculated in the same way but replacing the climate adjusted mortality and survival probability.

6.3 Reserves and Financial Impacts

For a contract with future benefit cash flows B_k and premium cash flows P_k (positive from the insurer's perspective), the prospective reserve (technical provision) at valuation time t for an individual aged x is

$$V^{(b)}(x,t) = \sum_{k>t} v^{k-t} \, \mathbb{E}^{(b)}[B_k - P_k \mid x, t] \, , \tag{21}$$

where the expectation is taken on the basis b using the cohort survival probabilities and (where relevant) death.

6.4 Illustrative Example: Data and Assumptions

Baseline mortality is taken from Eurostat EUROPOP2019 regional projections. We used mortality rates from `proj_19raasmr3` [2] and population weights from `proj_19rp3` [1], and computed sex-weighted rates for Bucharest (NUTS 3 code RO321). Contracts are issued at the start of the cohort and payment periods are reported in the tables. Adaptation is set to zero in all illustrative results, so the figures focus on the effect of temperature while keeping the rest of the framework unchanged.

Projections are available only up to the year 2100, so for $t > 2100$ we set the mortality rates and the temperature distribution equal to their 2100 values. This is a practical closure and may understate

the effects for young cohorts in 2050 who could experience post-2100 climate conditions. We also adopt the standard actuarial convention that $q_x = 1$ for ages older than 100, i.e., death occurs within the year. In our case, the limiting age ω is 100.

The numerical results reported in this subsection are point estimates, using the daily mean temperatures to compute the mortality multipliers. They are intended to establish the pipeline and to give an order of magnitude for the temperature effect. A full Monte Carlo implementation, with uncertainty intervals for mortality multipliers and EPVs, is left for future work.

Table 3: Values of $\ddot{a}_{60,2025}$ (whole-life annuity-due EPV) and $A_{60,2025}$ (whole-life insurance EPV), for a cohort aged 60 at year 2025, under alternative interest rates i and climate scenarios. At $i = 0\%$, the largest climate deltas are about -0.50% for $\ddot{a}_{60,2025}$ and $+0.21\%$ for $A_{60,2025}$ (RCP 8.5 vs. base).

	i	**Base**	**2.6**	**4.5**	**7.0**	**8.5**
$\ddot{a}_{60,2025}$	0%	24.596	24.587	24.585	24.584	24.474
	2%	18.934	18.930	18.929	18.928	18.862
	4%	15.139	15.136	15.136	15.135	15.094
$A_{60,2025}$	0%	0.966	0.966	0.966	0.967	0.968
	2%	0.614	0.614	0.614	0.614	0.616
	4%	0.411	0.411	0.411	0.411	0.413

Table 3 shows that interest dominates the temperature effect for this cohort. Moving from $i = 0\%$ to $i = 4\%$ changes $\ddot{a}_{60,2025}$ by approximately 9.5 units, whereas the largest climate spread is approximately 0.12. The same pattern holds for $A_{60,2025}$, with a rate-driven spread of about 0.560 and a climate spread of about 0.002. This scale gap reflects discounting because near-term cash flows receive much higher weight and the temperature effect enters mainly through distant-year mortality; higher interest rates therefore compress its present value. Demographic shifts tied to SSP narratives, such as migration, can move baseline mortality and cash flows far more than temperature alone, so we exclude those SSP-driven effects here to keep the temperature effect clear and avoid mixing sources of variation.

Table 4 is calculated at $i = 0\%$, so the EPV due to the annuity satisfies $\ddot{a}_{x,t} = \sum_{k\geq 0} {}_kp_{x,t} = 1 + e_{x,t}$, where $e_{x,t}$ is the curtate life expectancy. The baseline shift between 2025 and 2050 comes from Eurostat mortality improvement assumptions in the reference projections rather than climate. The temperature effect is modest. For $\ddot{a}_{40,2050}$, the value of RCP 7.0 is approximately 0.222 below baseline, or about -0.45%, while for insurance EPVs the greatest positive change occurs at age 20, where the increase in $A_{x,t}$

Table 4: Values of $\ddot{a}_{x,t}$ (whole-life annuity-due EPV) and $A_{x,t}$ (whole-life insurance EPV) by age x and valuation time t, with $i = 0\%$. The largest climate deltas are about -0.45% for $\ddot{a}_{40,2050}$ (RCP 7.0 vs. base) and $+1.10\%$ for $A_{20,2050}$ (RCP 7.0 vs. base).

Quantity	x	t	**Base**	**2.6**	**4.5**	**7.0**	**8.5**
$\ddot{a}_{x,t}$	20	2025	67.657	67.642	67.600	67.466	67.336
	20	2050	70.084	70.062	70.027	69.804	69.785
	40	2025	45.294	45.280	45.261	45.217	45.091
	40	2050	48.946	48.929	48.888	48.724	48.626
	60	2025	24.596	24.587	24.585	24.584	24.474
	60	2050	28.351	28.338	28.312	28.243	28.125
$A_{x,t}$	20	2025	0.922	0.922	0.923	0.929	0.930
	20	2050	0.909	0.910	0.911	0.919	0.918
	40	2025	0.947	0.947	0.948	0.950	0.953
	40	2050	0.916	0.916	0.917	0.924	0.925
	60	2025	0.966	0.966	0.966	0.967	0.968
	60	2050	0.935	0.935	0.936	0.939	0.943

is approximately 0.9–1.1% relative to baseline. The signs are opposite for annuities and assurances: higher mortality reduces annuity values and increases insurance values, so a balanced portfolio could offset part of the climate effect. Overall, the Bucharest example shows a small temperature effect on EPVs, yet the signal is systematic and still relevant for climate-risk sensitivity analysis. These magnitudes motivate the interpretation in the next section.

7. Interpretation and Scope

The objective of the methodology presented in this paper is to support a scenario-based analysis of how mortality assumptions, life tables, and related life-contingent liabilities may evolve under alternative future climate pathways. The framework is explicitly designed to assess the sensitivity to different temperature trajectories and adaptation assumptions. This paper analyses only the direct effect of temperature on mortality and translates this variation into the expected present value of simple insurance products.

Demographic scenarios in Shared Socioeconomic Pathways imply much wider variation, since mortality trends depend strongly on geopolitical and socioeconomic trajectories. In addition, the financial risk from changing interest rates is much higher than the direct effects of temperature on mortality when pricing insurance products.

The paper isolates the direct effect of temperature through multiplicative risk factors. These factors can be applied to any life table used for a given population subset and region.

As a rule of thumb, our initial calculation for the city of Bucharest implies that modifying a standard projected life table under RCP 7.0 (which is moderately pessimistic but feasible), the expected present value of annuities and life assurance needs to be modified by a factor between 0.5% and 1% (assuming no future discounting, i.e. essentially life expectancy). Other regions may exhibit larger effects, and a broader geographic analysis is left for future work.

While the direct temperature effect on EPVs is modest in isolation, the value of the framework lies in its scalability across regions, ages, and portfolios, and in its ability to integrate consistently with other climate- and demography-driven risk channels.

Climate change also affects mortality through channels beyond temperature, in particular cardiovascular disease and exposure to emissions. These channels are left for future work.

References

1 Eurostat. *Population on 1st January by age, sex and NUTS 3 region (EUROPOP2019)*. Eurostat Data Browser. Dataset code: proj_19rp3. 2020. DOI: 10.2908/PROJ_19RP3. URL: https://ec.europa.eu/eurostat/databrowser/view/proj_19rp3.

2 Eurostat. *Projected mortality rates by age, sex and NUTS 3 region (EUROPOP2019)*. Eurostat Data Browser. Dataset code: proj_19raasmr3. 2020. DOI: 10.2908/PROJ_19RAASMR3. URL: https://ec.europa.eu/eurostat/databrowser/view/proj_19raasmr3.

3 David Garcia-Leon et al. "Temperature-related mortality burden and projected change in 1368 European regions: a modelling study". In: *The Lancet Public Health* 9.10 (2024), e725–e735. DOI: 10.1016/S2468-2667(24)00179-8.

4 Antonio Gasparrini, Ben Armstrong, and Mike G Kenward. "Distributed lag non-linear models". In: *Statistics in Medicine* 29.21 (2010), pp. 2224–2234. DOI: 10.1002/sim.3940.

5 Antonio Gasparrini et al. "Projections of temperature-related excess mortality under climate change scenarios". In: *The Lancet Planetary Health* 1.9 (2017), e360–e367. DOI: 10.1016/S2542-5196(17)30156-0.

6 Hans Hersbach et al. "The ERA5 global reanalysis". In: *Quarterly journal of the royal meteorological society* 146.730 (2020), pp. 1999–2049. DOI: 10.1002/qj.3803.

7 Andrew Hinde. *Demographic methods*. Routledge, 2014. DOI: 10.4324/9780203784273.

8 Pierre Masselot et al. "Excess mortality attributed to heat and cold: a health impact assessment study in 854 cities in Europe". In: *The Lancet Planetary Health* 7.4 (2023), e271–e281. DOI: 10.1016/S2542-5196(23)00023-2.

9 Pierre Masselot et al. "Estimating future heat-related and cold-related mortality under climate change, demographic and adaptation scenarios in 854 European cities". In: *Nature Medicine* 31.4 (2025), pp. 1294–1302. DOI: 10.1038/s41591-024-03452-2.

10 National Institute of Statistics of Romania. *Romanian Demographic Yearbook*. 2024th ed. Anuarul Demografic al României, ediția 2024. Bucharest: National Institute of Statistics, 2024. URL: https://insse.ro/cms/en/content/demographic-yearbook-romania.

11 *NGFS Climate Scenarios for central banks and supervisors*. Tech. rep. Network for Greening the Financial System, 2024. URL: https://www.ngfs.net/en/publications-and-statistics/publications/ngfs-climate-scenarios-central-banks-and-supervisors.

12 Samuel H. Preston, Patrick Heuveline, and Michel Guillot. *Demography: Measuring and Modeling Population Processes*. Oxford: Blackwell Publishers, 2001.

13 Keywan Riahi et al. “The Shared Socioeconomic Pathways and their energy, land use, and greenhouse gas emissions implications: An overview”. In: *Global environmental change* 42 (2017), pp. 153–168. DOI: 10.1016/j.gloenvcha.2016.05.009.
14 Silvia Rizzi, Jutta Gampe, and Paul H.C. Eilers. “Efficient Estimation of Smooth Distributions From Coarsely Grouped Data”. In: *American Journal of Epidemiology* 182.2 (2015), pp. 138–147. DOI: 10.1093/aje/kwv020.
15 Jens Robben and Karim Barigou. *A Penalized Distributed Lag Non-Linear Lee-Carter Framework for Regional Weekly Mortality Forecasting*. 2025. DOI: 10.48550/arXiv.2509.24087. arXiv: 2509.24087 [stat.AP].
16 Detlef P Van Vuuren et al. “The representative concentration pathways: an overview”. In: *Climatic change* 109.1 (2011), p. 5. DOI: 10.1007/s10584-011-0148-z.
17 Nan Zhou et al. “On the definition of an actuarial climate index for the Iberian Peninsula”. In: *Anales del Instituto de Actuarios Españoles* 29 (2023), pp. 37–59. DOI: 10.26360/2023_3.